ELSEVIER

Journal of Membrane Science 107 (1995) 1–21

journal of MEMBRANE SCIENCE

The solution-diffusion model: a review

J.G. Wijmans, R.W. Baker *

Membrane Technology and Research, Inc., 1360 Willow Road, Suite 103, Menlo Park, CA 194025-1516, USA

Received 28 December 1994; accepted 3 April 1995

Abstract

The solution-diffusion model has emerged over the past 20 years as the most widely accepted explanation of transport in dialysis, reverse osmosis, gas permeation, and pervaporation. In this paper we will derive the phenomenological equations for transport in these processes using the solution-diffusion model and starting from the fundamental statement that flux is proportional to a gradient in chemical potential. The direct and indirect evidence for the model's validity will then be presented, together with a brief discussion of the transition between a solution-diffusion membrane and a pore-flow membrane seen in nanofiltration membranes and some gas permeation membranes.

Keywords: Solution-diffusion model; Transport equations; Pore-flow; Membrane mechanisms

1. Introduction

The principal property of membranes used in separation applications is the ability to control the permeation of different species. Two models are used to describe this permeation process. The first is the solution-diffusion model, in which permeants dissolve in the membrane material and then diffuse through the membrane down a concentration gradient. A separation is achieved between different permeants because of differences in the amount of material that dissolves in the membrane and the rate at which the material diffuses through the membrane. The second is the pore-flow model, in which permeants are separated by pressure-driven convective flow through tiny pores. A separation is achieved between different permeants because one of the permeants is excluded (filtered) from some of the pores in the membrane through which other permeants move. Both models were proposed in the nineteenth century, but the pore-flow model, because it was closer to normal physical experience, was more popular until the mid-1940s. However, during the 1940s, the solution-diffusion model was used to explain transport of gases across polymeric films. This use of the solution-diffusion model was relatively uncontroversial, but the transport mechanism in reverse osmosis membranes was a hotly debated issue in the 1960s and early 1970s [1–16]. By 1980, however, the proponents of solution-diffusion had carried the day; currently only a few die-hard pore-flow modelers use this approach to rationalize reverse osmosis.

In this review, the assumptions behind these two membrane models are discussed, and the appropriate transport equations for dialysis, reverse osmosis, gas permeation, and pervaporation are derived using the solution-diffusion model. We show that these diverse processes can all be described by a single unified approach based on the solution-diffusion model. The experimental evidence that supports the solution-dif-

* Corresponding author. Phone: (415) 328-2228. Fax: (415) 328-6580.

SSDI 0376-7388(95)00102-6

fusion model as it applies to these processes is reviewed, and the transition region between pure solution-diffusion and pure pore-flow membranes is discussed.

2. Concentration and pressure gradients in membranes

The starting point for the mathematical description of permeation in all membranes is the proposition, solidly based in thermodynamics, that the driving forces of pressure, temperature, concentration, and electromotive force are interrelated and that the overall driving force producing movement of a permeant is the gradient in its chemical potential. Thus, the flux, J_i, of a component, i, is described by the simple equation

$$J_i = -L_i \frac{d\mu_i}{dx} \tag{1}$$

where $d\mu_i/dx$ is the gradient in chemical potential of component i and L_i is a coefficient of proportionality (not necessarily constant) linking this chemical potential driving force with flux [1]. All the common driving forces, such as gradients in concentration, pressure, temperature, and electromotive force, can be reduced to chemical potential gradients, and their effect on flux expressed by this equation. This approach is extremely useful, because many processes involve more than one driving force, for example, pressure and concentration in reverse osmosis. Restricting ourselves to driving forces generated by concentration and pressure gradients, the chemical potential is written as

$$d\mu_i = RTd\ln(\gamma_i c_i) + v_i dp \tag{2}$$

where c_i is the molar concentration (mol/mol) of component i, γ_i is the activity coefficient linking concentration with activity, p is the pressure, and v_i is the molar volume of component i.

In incompressible phases, such as a liquid or a solid membrane, volume does not change with pressure. Integrating Eq. (2) with respect to concentration and pressure gives

$$\mu_i = \mu_i^o + RT\ln(\gamma_i c_i) + v_i(p - p_i^o) \tag{3}$$

[1] In this paper we ignore the cross coefficients of irreversible thermodynamics.

where μ_i^o is the chemical potential of pure i at a reference pressure p_i^o.

In compressible gases, the molar volume changes with pressure; using the ideal gas laws in integrating Eq. (2) gives

$$\mu_i = \mu_i^o + RT\ln(\gamma_i c_i) + RT\ln\frac{p}{p_i^o} \tag{4}$$

To ensure that the reference chemical potential μ_i^o is identical in Eqs. (3) and (4), the reference pressure p_i^o is defined as the saturation vapor pressure of i, $p_{i_{sat}}$. Eqs. (3) and (4) can then be rewritten as

$$\mu_i = \mu_i^o + RT\ln(\gamma_i c_i) + v_i(p - p_{i_{sat}}) \tag{5}$$

for incompressible liquids and the membrane phase, and as

$$\mu_i = \mu_i^o + RT\ln(\gamma_i c_i) + RT\ln\frac{p}{p_{i_{sat}}} \tag{6}$$

for compressible gases.

A number of assumptions must be made to define any model of permeation. Usually, the first assumption governing transport through membranes is that the fluids on either side of the membrane are in equilibrium with the membrane material at the interface. This assumption means that there is a continuous gradient in chemical potential from one side of the membrane to the other. It is implicit in this assumption that the rates of absorption and desorption at the membrane interface are much higher than the rate of diffusion through the membrane. This appears to be the case in almost all membrane processes, but may fail, for example, in transport processes involving chemical reactions, such as facilitated transport, or in diffusion of gases through metals, where interfacial absorption can be slow.

The solution-diffusion and pore-flow models differ in the way the chemical potential gradient in the membrane phase is expressed [8,9,15,17]:

- The solution-diffusion model assumes that the pressure within a membrane is uniform and that the chemical potential gradient across the membrane is expressed only as a concentration gradient.
- The pore-flow model assumes that the concentrations of solvent and solute within a membrane are uniform and that the chemical potential gradient across the membrane is expressed only as a pressure gradient.

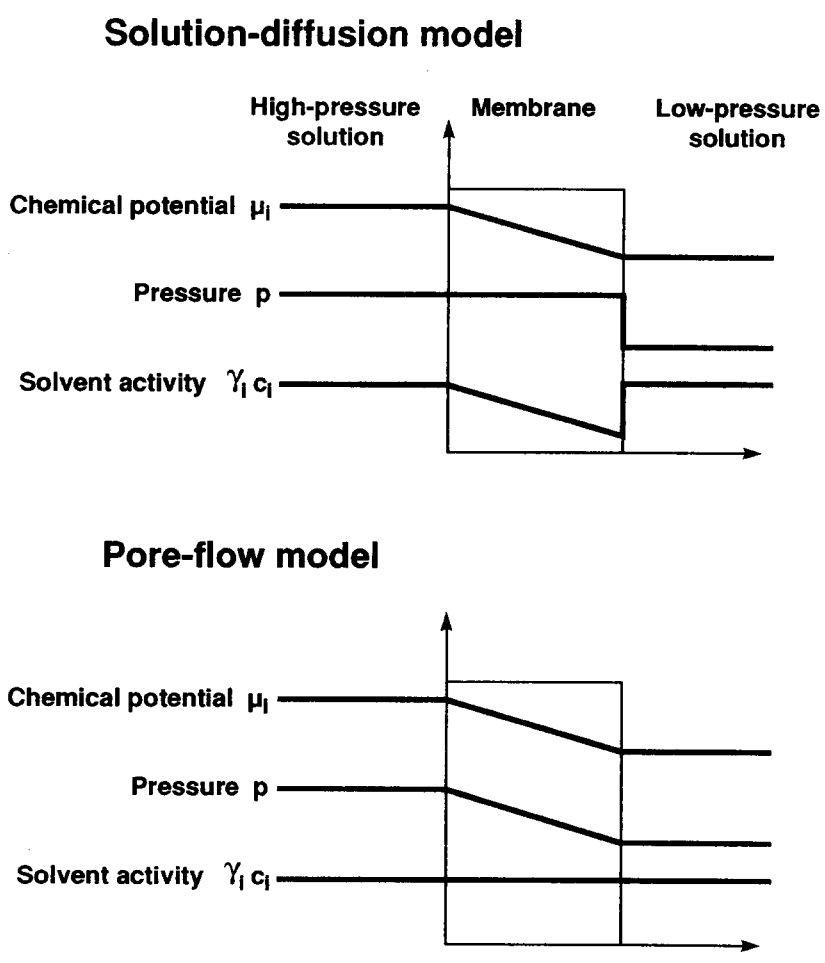

Fig. 1. Pressure-driven permeation of a one-component solution through a membrane according to solution-diffusion and pore-flow transport models[2].

The consequences of these two assumptions are illustrated in Fig. 1, which compares pressure-driven permeation of a one-component solution by solution-diffusion and by pore-flow [2]. In both models, the difference in pressure across the membrane $(p_o - p_\ell)$ produces a gradient in chemical potential according to Eqs. (1) and (2). In the pore-flow model, the pressure difference produces a smooth gradient in pressure through the membrane, but the solvent activity $(\gamma_i c_i)$ remains constant within the membrane. The solution-diffusion model on the other hand assumes that, when a pressure is applied across a dense membrane, the pressure everywhere within the membrane is constant at the high-pressure value. This assumes, in effect, that solution-diffusion membranes transmit pressure in the same way as liquids. Consequently, the pressure difference across the membranes is expressed as a concentration gradient within the membrane, with Eqs. (1) and (2) providing the mathematical link between pressure and concentration.

Consider the pore-flow model first. Combining Eqs. (1) and (2) in the absence of a concentration gradient in the membrane gives

$$J = -L\upsilon\frac{dp}{dx} \tag{7}$$

[2] At this point it is worth noting that, in the pore-flow model, the pressure gradient exists only in the fluid-filled pores. No pressure gradient exists within the membrane matrix material, which is at the feed pressure throughout. The existence of two pressure gradients is a consequence of the two-phase nature of the pore-flow model.

This equation can be integrated across the membrane to give Darcy's law

$$J=\frac{k(p_o-p_\ell)}{\ell} \tag{8}$$

where k is the Darcy's law coefficient, equal to Lv, and ℓ is the membrane thickness.

In the solution-diffusion model, the pressure within the membrane is constant at the high-pressure value (p_o), and the gradient in chemical potential across the membrane is expressed as a smooth gradient in solvent activity ($\gamma_i c_i$). The flow that occurs down this gradient is again expressed by Eq. (1), but, because no pressure gradient exists within the membrane, Eq. (1) can be written, by combining Eqs. (1) and (2), as

$$J_i=-\frac{RTL_i}{c_i}\cdot\frac{dc_i}{dx} \tag{9}$$

This has the same form as Fick's law where the term RTL_i/c_i can be replaced by the diffusion coefficient D_i. Thus:

$$J_i=-D_i\frac{dc_i}{dx} \tag{10}$$

and integrating over the thickness of the membrane then gives [3]

$$J_i=\frac{D_i(c_{io(m)}-c_{i\ell(m)})}{\ell} \tag{11}$$

2.1. Osmosis according to the solution-diffusion model

Using osmosis as an example, we can discuss concentration and pressure gradients according to the two models in a somewhat more complex situation. Consider the application of the solution-diffusion model to osmotic membranes first. The activity, pressure, and chemical potential gradients within this type of membrane are illustrated in Fig. 2.

[3] In the equations that follow, the terms i and j represent components of a solution, and the terms o and ℓ represent the positions of the feed and permeate interfaces, respectively, of the membrane. Thus the term c_{i_o} represents the concentration of component i in the fluid (gas or liquid) in contact with the membrane at the feed interface. The subscript m is used to represent the membrane phase. Thus, $c_{i_{o(m)}}$ is the concentration of component i in the membrane at the feed interface (point o).

Fig. 2(a) shows a semipermeable membrane separating a salt solution from pure solvent. The pressure is the same on both sides of the membrane. For simplicity, the gradient of salt (component j) is not shown in this figure, but we assume the membrane to be very selective, so the concentration of salt within the membrane is small. The difference in concentration across the membrane results in a continuous, smooth gradient in chemical potential of the water (component i) across the membrane from μ_{i_ℓ} on the water side to μ_{i_o} on the salt side. The pressure within and across the membrane is constant (i.e. $p_o=p_m=p_\ell$), and the solvent activity gradient ($\gamma_i c_i$) falls continuously from the pure water (solvent) side to the saline (solution) side of the membrane. As a result, water passes across the membrane from right to left.

Fig. 2(b) shows the situation at the point of osmotic equilibrium, when sufficient pressure has been applied to the saline side of the membrane to bring the flow across the membrane to zero. As shown in Fig. 2(b), the pressure within the membrane is assumed to be constant at the high-pressure value p_o. There is a discontinuity in pressure at the permeate side of the membrane, where the pressure abruptly falls from p_o to p_ℓ, the pressure on the solvent side of the membrane. This pressure difference (p_o-p_ℓ) is equal to the osmotic pressure difference $\Delta\pi$. Equating the chemical potential on either side of the permeate interface, from Eq. (5) we obtain

$$RT\ln(\gamma_{i\ell(m)}c_{i\ell(m)})-RT\ln(\gamma_{i\ell}c_{i\ell})=-v_i(p_o-p_\ell) \tag{12}$$

We can also define $\Delta(\gamma_i c_i)$ by

$$\gamma_{i\ell(m)}c_{i\ell(m)}=(\gamma_{i\ell}c_{i\ell})-\Delta(\gamma_i c_i) \tag{13}$$

and, since $(\gamma_{i\ell}c_{i\ell})\approx 1$, it follows, on substituting Eq. (13) into Eq. (12), that

$$RT\ln[1-\Delta(\gamma_i c_i)]=-v_i(p_o-p_\ell) \tag{14}$$

Since $\Delta(\gamma_i c_i)$ is small, Eq. (14) reduces to

$$\Delta(\gamma_i c_i)=\frac{v_i(p_o-p_\ell)}{RT}=\frac{v_i\Delta\pi}{RT} \tag{15}$$

Thus, the pressure difference, $(p_o-p_\ell)=\Delta\pi$, across the membrane balances the solvent activity difference $\Delta(\gamma_i c_i)$ across the membrane, and the flow is zero.

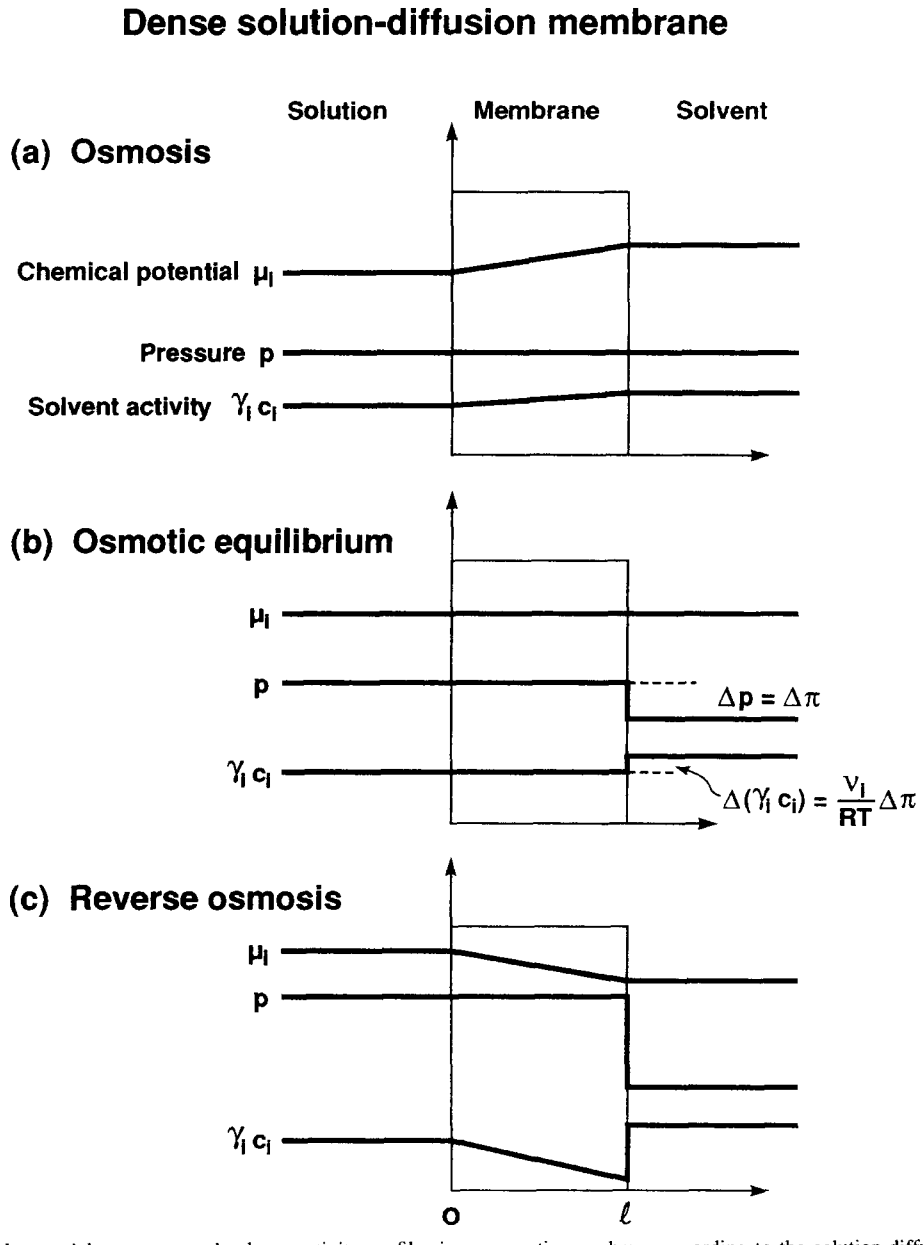

Fig. 2. Chemical potential, pressure, and solvent activity profiles in an osmotic membrane according to the solution-diffusion model. The pressure in the membrane is uniform and equal to the high-pressure value, so the chemical potential gradient within the membrane is expressed as a concentration gradient.

If a pressure higher than the osmotic pressure is applied to the feed side of the membrane, as shown in Fig. 2(c), then the solvent activity difference across the membrane increases further, resulting in a flow from left to right. This is the process of reverse osmosis.

2.2. *Osmosis according to the pore-flow model*

The activity, chemical potential, and pressure gradients within an osmotic membrane according to the pore-flow model are illustrated in Fig. 3. This figure is the pore-flow equivalent of Fig. 2 and shows the gra-

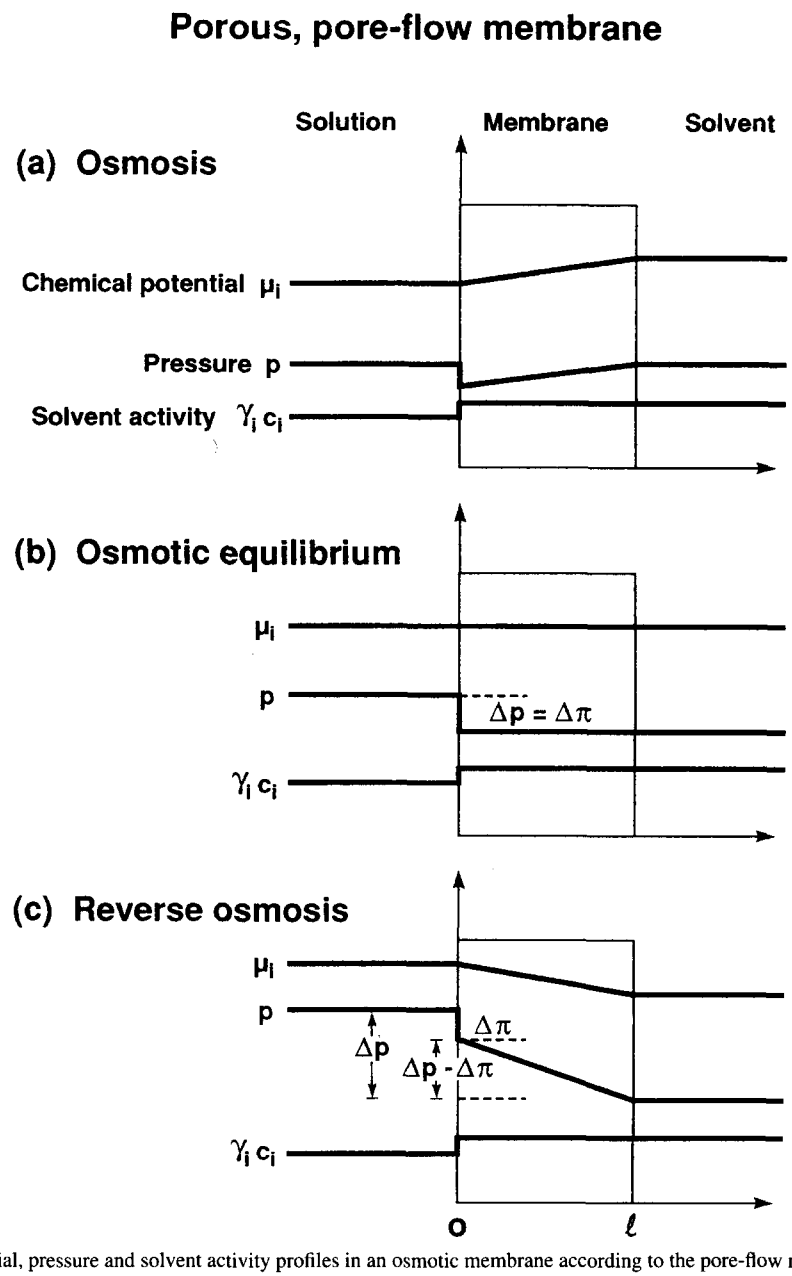

Fig. 3. Chemical potential, pressure and solvent activity profiles in an osmotic membrane according to the pore-flow model. The concentration within the membrane is assumed to be uniform, so the chemical potential gradient in the membrane is expressed as a pressure gradient.

dients when a very selective semipermeable porous membrane separates a solute solution from a pure solvent.

Fig. 3(a) shows the case of normal osmosis with no concentration gradient within the membrane but a pressure gradient induced by the concentration difference between the solutions on either side of the membrane.

Fig. 3(b) shows the situation at the point of osmotic equilibrium, when a sufficient pressure has been applied to the solute solution side of the membrane to bring the flow across the membrane to zero. As in Fig. 2(b), the pressure gradient within the membrane is at the permeate-side value, and there is a discontinuity in pressure at the feed side interface where the

pressure difference Δp across the membrane occurs. This pressure difference $(p_o - p_\ell)$ is equal to the osmotic pressure $\Delta\pi$.

When a pressure higher than the osmotic pressure is applied to the feed side of the membrane, as shown in Fig. 3(c), the pressure gradient within the membrane increases further, and solvent flow is from left to right.

The important conclusion illustrated in Fig. 1 Fig. 2 Fig. 3 is that, although the fluids on either side of a membrane may be at different pressures and concentrations, within a perfect solution-diffusion membrane only a concentration gradient exists. Flow through this type of membrane is expressed by Fick's law, Eq. (11). Within a perfect pore-flow membrane, only a pressure gradient exists. Flow through this type of membrane is expressed by Darcy's law, Eq. (8). In the next section, the appropriate quantitative expressions describing flow through solution-diffusion membranes are derived by calculating the concentration gradient within the membrane and then substituting this gradient into the Fick's law expression.

3. Application of the solution-diffusion model to specific processes

In this section, the appropriate equations for the solution-diffusion model for transport in dialysis, reverse osmosis, gas permeation, and pervaporation membranes are derived. The resulting equations linking the driving forces of pressure and concentration with flow are then shown to be consistent with experimental observations.

The general approach is to use the first assumption of the solution-diffusion model, namely, that the chemical potential of the feed and permeate fluids are in equilibrium with the adjacent membrane surfaces. From this assumption, the chemical potential in the fluid and membrane phases can be equated using the appropriate expressions for chemical potential given in Eqs. (5) and (6). By rearranging these equations, the concentration of the differing species in the membrane at the fluids interface $c_{i_{o(m)}}$ and $c_{i_{\ell(m)}}$ can be obtained in terms of the pressure and composition of the feed and permeate fluids. These values for $c_{i_{o(m)}}$ and $c_{i_{\ell(m)}}$ can then be substituted into the Fick's law expression, Eq. (11), to give the transport equation for the particular process.

3.1. Dialysis

To illustrate the application of the general procedure described above, we will derive the appropriate solution-diffusion model transport equation for dialysis, which is the simplest application of the model because only concentration gradients are involved. In dialysis, a membrane is used to separate two solutions of different compositions. The concentration gradient across the membrane causes a flow of solute and solvent from one side of the membrane to the other.

Following the general procedure described above, equating the chemical potentials at the feed side interface of the membrane gives

$$\mu_{i_o} = \mu_{i_{o(m)}} \tag{16}$$

Substituting the expression for the chemical potential of incompressible fluids from Eq. (5) gives

$$\mu_i^o + RT\ln(\gamma_{i_o} c_{i_o}) + v_i(p_o - p_{i_{sat}}) = \mu_i^o + RT\ln(\gamma_{i_{o(m)}} c_{i_{o(m)}}) + v_{i_{o(m)}}(p_o - p_{i_{sat}}) \tag{17}$$

which leads to

$$\ln(\gamma_{i_o} c_{i_o}) = \ln(\gamma_{i_{o(m)}} c_{i_{o(m)}}) \tag{18}$$

and, thus

$$c_{i_{o(m)}} = \frac{\gamma_{i_o}}{\gamma_{i_{o(m)}}} \cdot c_{i_o} \tag{19}$$

The ratio of activity coefficients $\gamma_{i_o}/\gamma_{i_{o(m)}}$ is the sorption coefficient, K_i, and Eq. (19) becomes

$$c_{i_{o(m)}} = K_i \cdot c_{i_o} \tag{20}$$

On the permeate side of the membrane, the same procedure can be followed, leading to an equivalent expression

$$c_{i_{\ell(m)}} = K_i \cdot c_{i_\ell} \tag{21}$$

The concentrations of permeant within the membrane phase at the two interfaces can then be substituted from Eqs. (20) and (21) into the Fick's law expression, Eq. (11), to give the familiar expression describing permeation through dialysis membranes

$$J_i = \frac{D_i K_i}{\ell}(c_{i_o} - c_{i_\ell}) \tag{22}$$

The product $D_i \cdot K_i$ is normally referred to as the permeability coefficient, P_i. For many systems, D_i, K_i and

thus P_i are concentration dependent. Thus, Eq. (22) implies the use of values for D_i, K_i and P_i that are averaged over the membrane thickness.

The permeability coefficient P_i is often treated as a pure materials constant, depending only on the permeant and the membrane material, but, in fact, the nature of the solvent used in the liquid phase is also important. From Eq. (19), P_i can be written as

$$P_i = D_i \cdot \gamma_i / \gamma_{i(m)} \tag{23}$$

It is the presence of the term γ_i that makes the permeability coefficient a function of the solvent used as the liquid phase. Some experimental data illustrating this effect are shown in Fig. 4 [18], which is a plot of the progesterone flux times the membrane thickness, $J_i \cdot \ell$, against the concentration difference across the membrane, $(c_{i_o} - c_{i\ell})$. From Eq. (22), the slope of this line is the permeability, P_i. Three sets of permeation experiments are reported, in which the solvent used to dissolve the progesterone is water, silicone oil, and polyethylene glycol MW600 (PEG 600), respectively. The permeability calculated from these plots varies from 9.5×10^{-7} cm^2/s for water to 6.5×10^{-10} cm^2/s for PEG 600. This difference reflects the activity term γ_i in Eq. 23. However, the product of permeability and the progesterone saturation concentration of the solute, $P_i c_{\text{sat}}$, is a constant as shown in Fig. 4(d). This result is also in agreement with Eq. (23), which combined with the approximation

$$\gamma_i = \frac{1}{c_{\text{sat}}} \tag{24}$$

yields

$$\frac{P_i}{\gamma_i} = P_i c_{\text{sat}} = \frac{D_i}{\gamma_{i(m)}} \tag{25}$$

The term $D_i/\gamma_{i(m)}$ and therefore the term $P_i c_{\text{sat}}$ are determined solely by the permeant and the membrane material and are thus independent of the liquid phase surrounding the membrane.

3.2. Reverse osmosis

Reverse osmosis and normal osmosis (dialysis) are directly related processes. In simple terms, if a permselective membrane (i.e. a membrane freely permeable to water, but much less permeable to salt) is used to separate a salt solution from pure water, water will pass through the membrane from the pure-water side of the membrane into the side less concentrated in water (salt side). This process is called normal osmosis. If a hydrostatic pressure is applied to the salt side of the membrane, the flow of water can be retarded and, when the applied pressure is sufficient, the flow ceases. The hydrostatic pressure required to stop the water flow is called the osmotic pressure ($\Delta\pi$). If pressures greater than the osmotic pressure are applied to the salt side of the membrane, then the flow of water is reversed, and water begins to flow from the salt solution to the pure water side of the membrane. This process is called reverse osmosis and is an important method of producing pure water from salt solutions.

In reverse osmosis, we are usually dealing with two components, water (i), and salt (j). Following the general procedure, the chemical potentials at both sides of the membrane are first equated. At the feed interface, the pressure in the feed solution and within the membrane are identical [as shown in Fig. 2(b)]. Equating the chemical potentials at this interface gives the same expression as in dialysis [cf. Eq. (20)]

$$c_{i_{o(m)}} = K_i \cdot c_{i_o} \tag{26}$$

At the permeate interface, a pressure difference exists [as shown in Fig. 2(b)] from p_o within the membrane to p_ℓ in the permeate solution. Equating the chemical potentials across this interface gives

$$\mu_{i\ell} = \mu_{i\ell(m)} \tag{27}$$

Substituting the appropriate expression for the chemical potential of an incompressible fluid [Eq. (5)] yields

$$\mu_i^o + RT\ln(\gamma_{i\ell} c_{i\ell}) + v_i(p_\ell - p_{i_{\text{sat}}}) = \mu_i^o + RT\ln(\gamma_{i\ell(m)} c_{i\ell(m)}) + v_i(p_o - p_{i_{\text{sat}}}) \tag{28}$$

which leads to

$$\ln(\gamma_{i\ell} c_{i\ell}) = \ln(\gamma_{i\ell(m)} c_{i\ell(m)}) + \frac{v_i(p_o - p_\ell)}{RT} \tag{29}$$

Rearranging and substituting for the sorption coefficient, K_i, gives the expression

$$c_{i\ell(m)} = K_i \cdot c_{i\ell} \cdot \exp\left(\frac{-v_i(p_o - p_\ell)}{RT}\right) \tag{30}$$

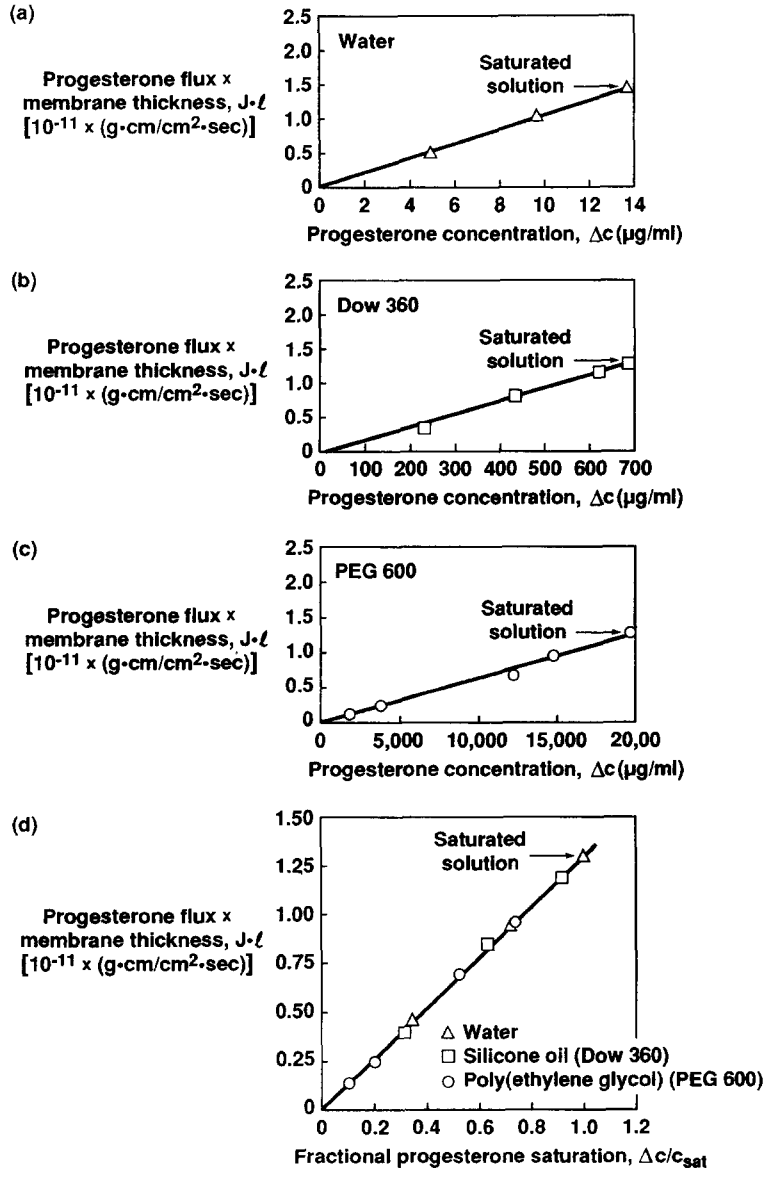

Fig. 4. Permeation of progesterone through polyethylene vinyl acetate films. The thickness-normalized progesterone flux ($J_i \cdot \ell$) is plotted against the progesterone concentration across the membrane, Δc [18]. The solvent phase used to dissolve the progesterone is (a) water, (b) silicone oil, and (c) polyethylene glycol (PEG 600). Because of the different solubilities of progesterone in these solvents, the permeabilities calculated from these data through Eq. (22) vary 1000-fold. All the data can be rationalized onto a single curve by plotting the thickness-normalized flux against fractional progesterone saturation as described in the text and shown in (d). The slope of this line $P_i c_{sat}$ or $D_i/\gamma_{i(m)}$, is a materials property dependent only on the membrane material and the permeant, and is independent of the fluid used as the solvent.

The expressions for the concentrations within the membrane at the interface in Eqs. (26) and (30) can now be substituted into the Fick's law expression, Eq. (11), to yield

$$J_i = \frac{D_i K_i}{\ell}\left[c_{i_o} - c_{i_\ell} \exp\left(\frac{-v_i(p_o - p_\ell)}{RT}\right)\right] \tag{31}$$

Eq. (31) and the equivalent expression for component j give the water flux and the salt flux across the reverse

osmosis membrane in terms of the pressure and concentration difference across the membrane. However, Eq. (31) can be simplified further. Consider the water flux first. At the point at which the applied hydrostatic pressure balances the water activity gradient, that is, the point of osmotic equilibrium in Fig. 2, the flux of water across the membrane is zero. Eq. (31) becomes

$$J_i = 0 = \frac{D_i K_i}{\ell}\left[c_{i_o} - c_{i_\ell} \exp\left(\frac{-v_i(\Delta\pi)}{RT}\right)\right] \tag{32}$$

and, thus,

$$c_{i_\ell} = c_{i_o} \exp\left(\frac{v_i(\Delta\pi)}{RT}\right) \tag{33}$$

At hydrostatic pressures higher than $\Delta\pi$, Eqs. (33) and (31) can be combined to yield

$$J_i = \frac{D_i K_i c_{i_o}}{\ell}\left[1 - \exp\left(\frac{-v_i[(p_o - p_\ell) - \Delta\pi]}{RT}\right)\right] \tag{34}$$

or

$$J_i = \frac{D_i K_i c_{i_o}}{\ell}\left[1 - \exp\left(\frac{-v_i(\Delta p - \Delta\pi)}{RT}\right)\right] \tag{35}$$

where Δp is the difference in hydrostatic pressure across the membrane $(p_o - p_\ell)$. A trial calculation shows that the term $-v_i(\Delta p - \Delta\pi)/RT$ is small under the normal conditions of reverse osmosis. For example, when $\Delta p = 100$ atm, $\Delta\pi = 10$ atm, and $v_i = 18$ cm^3, the term $v_i(\Delta p - \Delta\pi)/RT$ is about 0.06. Under these conditions, the simplification $1 - \exp(x) \rightarrow x$ as $x \rightarrow 0$ can be used, and Eq. (29) can be written to a very good approximation as

$$J_i = \frac{D_i K_i c_{i_o} v_i(\Delta p - \Delta\pi)}{\ell RT} \tag{36}$$

This equation can be simplified to

$$J_i = A(\Delta p - \Delta\pi) \tag{37}$$

where A is a constant equal to the term $D_i K_i c_{i_o} v_i / \ell RT$. In the reverse osmosis literature, the constant A is usually called the water permeability constant.

Similarly, a simplified expression for the salt flux, J_j, through the membrane can be derived, starting with the equivalent to Eq. (31):

$$J_j = \frac{D_j K_j}{\ell}\left[c_{j_o} - c_{j_\ell} \exp\left(\frac{-v_j(p_o - p_\ell)}{RT}\right)\right] \tag{38}$$

Because the term $-v_j(p_o - p_\ell)/RT$ is small, the exponential term in Eq. (38) is close to one, and Eq. (38) can then be written as

$$J_j = \frac{D_j K_j}{\ell}(c_{j_o} - c_{j_\ell}) \tag{39}$$

or

$$J_j = B(c_{j_o} - c_{j_\ell}) \tag{40}$$

where B is usually called the salt permeability constant and has the value

$$B = \frac{D_j K_j}{\ell} \tag{41}$$

Predictions of salt and water transport can be made from this application of the solution-diffusion model to reverse osmosis (first derived by Merten and co-workers [13,14]). According to Eq. (37), the water flux through a reverse osmosis membrane remains small up to the osmotic pressure of the salt solution and then increases with applied pressure, whereas according to Eq. (40), the salt flux is essentially independent of pressure. Some typical results are shown in Fig. 5. Also shown in this figure is a term called the rejection coefficient, $\mathbb{R}$, which is defined as

$$\mathbb{R} = \left(\frac{1 - c_{j_\ell}}{c_{j_o}}\right) \times 100\% \tag{42}$$

The rejection coefficient is a measure of the ability of the membrane to separate salt from the feed solution.

For a perfectly permselective membrane, $c_{j_\ell} = 0$ and $\mathbb{R} = 100\%$, and for a completely unselective membrane, $c_{j_\ell} = c_{j_o}$ and $\mathbb{R} = 0\%$. The rejection coefficient increases with applied pressure as shown in Fig. 5, because the water flux increases with pressure, but the salt flux does not.

As well as predicting the general form of the salt and water transport through reverse osmosis membranes, the solution-diffusion model has also been used by many workers to obtain diffusion and partition coefficient data. These data appear to be self-consistent and reasonable, based on diffusion coefficient data from gas separation and pervaporation.

3.3. Gas separation

In gas separation, a gas mixture at a pressure p_o is applied to the feed side of the membrane, while the

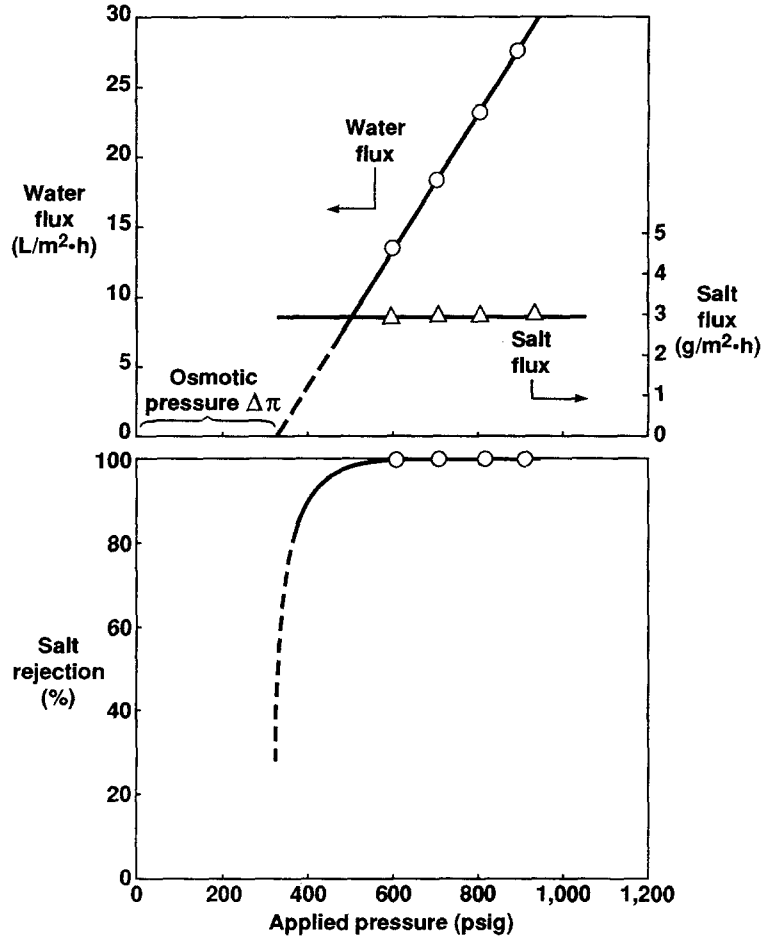

Fig. 5. Flux and rejection data for a model seawater solution (3.5% sodium chloride) in a good quality reverse osmosis membrane (FilmTec Corp., FT30 membrane) as a function of pressure. The salt flux, in accordance with Eq. (40), is essentially constant and independent of pressure. The water flux, in accordance with Eq. (37), increases with pressure, and, at zero flux, meets the pressure axis at the osmotic pressure of sea water ~350 psi.

permeate gas at a lower pressure p_ℓ is removed from the downstream side of the membrane. As before, the starting point for the derivation of the gas separation transport equation is to equate the chemical potentials on either side of the gas/membrane interface. This time, however, the chemical potential for the gas phase is given by Eq. (6) for a compressible fluid, whereas Eq. (5) for an incompressible medium is applied to the membrane phase. Substitution of these equations into Eq. (16) at the gas/membrane feed interface yields

$$\mu_i^o + RT\ln(\gamma_{i_o} c_{i_o}) + RT\ln\frac{p_o}{p_{i_{sat}}} = \mu_i^o + RT\ln(\gamma_{i_{o(m)}} c_{i_{o(m)}}) + v_i(p_o - p_{i_{sat}}) \tag{43}$$

which rearranges to

$$c_{i_{o(m)}} = \frac{\gamma_i}{\gamma_{i_{o(m)}}} \cdot \frac{p_o}{p_{i_{sat}}} \cdot c_{i_o} \exp\left(\frac{-v_i(p_o - p_{i_{sat}})}{RT}\right) \tag{44}$$

Because the exponential term is again very close to one [4], even for very large pressures p_o, Eq. (44) reduces to

$$c_{i_{o(m)}} = \frac{\gamma_{i_o} c_{i_o}}{\gamma_{i_{o(m)}}} \cdot \frac{p_o}{p_{i_{sat}}} \tag{45}$$

The term $c_{i_o} \cdot p_o$ is the partial pressure of i in the feed gas, p_{i_o}. Eq. (45) then simplifies to

$$c_{i_{o(m)}} = \frac{\gamma_{i_o}}{\gamma_{i_{o(m)}}} \cdot \frac{p_{i_o}}{p_{i_{sat}}} \tag{46}$$

The term $\gamma_{i_o}/(p_{i_{sat}} \cdot \gamma_{i_{o(m)}})$ is the sorption coefficient K_i^G [5], thus, the concentration of component i at the feed interface of the membrane can be written as

$$c_{i_{o(m)}} = K_i^G \cdot p_{i_o} \tag{47}$$

In exactly the same way, the concentration of component i at the membrane/permeate interface can be shown to be

$$c_{i_{\ell(m)}} = K_i^G p_{i_\ell} \tag{48}$$

Combining Eqs. (45) and (46) with the Fick's law expression, Eq. (11), then gives

$$J_i = \frac{D_i K_i^G (p_{i_o} - p_{i_\ell})}{\ell} \tag{49}$$

The product $D_i K_i^G$ is often abbreviated to a permeability coefficient, P_i^G, leading to the familiar expression

$$J_i = \frac{P_i^G (p_{i_o} - p_{i_\ell})}{\ell} \tag{50}$$

Eq. (50) is widely used to accurately and predictably rationalize the properties of gas permeation membranes.

It might be thought that the derivation leading to Eq. (50) is a long-winded way of arriving at a trivial result. However, this derivation explicitly clarifies the assumptions behind this equation. First, there is a gradient in concentration within the membrane but no gradient in pressure. Second, the absorption of a component into the membrane is proportional to its activity in the adjacent gas but is independent of the total gas pressure. This is related to the approximation made in Eq. (42), in which the Poynting correction was assumed to be one.

The permeability coefficient P_i^G can be written as

$$P_i^G = \frac{D_i \cdot \gamma_i}{\gamma_{i(m)} \cdot p_{i_{sat}}} \tag{51}$$

Eq. (51) is not a commonly used expression for gas-phase membrane permeability, but it is interesting because it shows that large permeability coefficients are obtained for compounds with a large diffusion coefficient (D_i), a limited affinity for the gas phase (high γ_i), a high affinity for the membrane material (small $\gamma_{i(m)}$), and a low saturation vapor pressure ($P_{i_{sat}}$). P_i^G is close to being a materials constant, relatively independent of the composition and pressure of the feed and permeate gases because gas-phase activity coefficients, γ_i, are usually close to unity. This is in sharp contrast to the permeability constant for liquids as described in the discussion centered on Fig. 4 earlier, but, even for gases, the concept of permeability as a materials constant must be treated with caution. For example, the permeability of vapors at partial pressures close to saturation often increases substantially with increasing partial pressure. This effect is commonly ascribed to plasticization and other effects of the permeant on the membrane changing D_i and $\gamma_{i(m)}$ in Eq. (51). However, significant deviations from ideality of the vapor's activity coefficient can also occur at high partial pressures.

Eq. (51) is also a useful way of rationalizing the effect of molecular weight on permeability. The permeant's saturation vapor pressure $p_{i_{sat}}$ and diffusion coefficient both decrease with increasing molecular weight creating competing effects on the permeability coefficient. In glassy polymers, the decrease in diffusion coefficient far outweighs other effects, and permeabilities fall significantly as molecular weight increases [19]. In rubbery polymers, on the other hand, the two effects are more balanced. For molecular weights up to 100, permeability generally increases

[4] While evaluating this exponential term (the Poynting correction), it is important to recognize that v_i is not the molar volume of i in the gas phase, but the molar volume of i dissolved in the membrane material, which is approximately equal to the molar volume of liquid i.

[5] The superscripts G and L are used here and later in Eq. (58) to distinguish between the liquid-phase sorption coefficient K_i^L defined by Eq. (20) and the gas-phase coefficient K_i^G defined by Eq. (47). Similarly, we will use P_i^G for the permeability coefficient for gases to distinguish from P_i^L for liquids. P_i^G and P_i^L have different dimensions but can be easily interconverted as shown in the pervaporation section that follows.

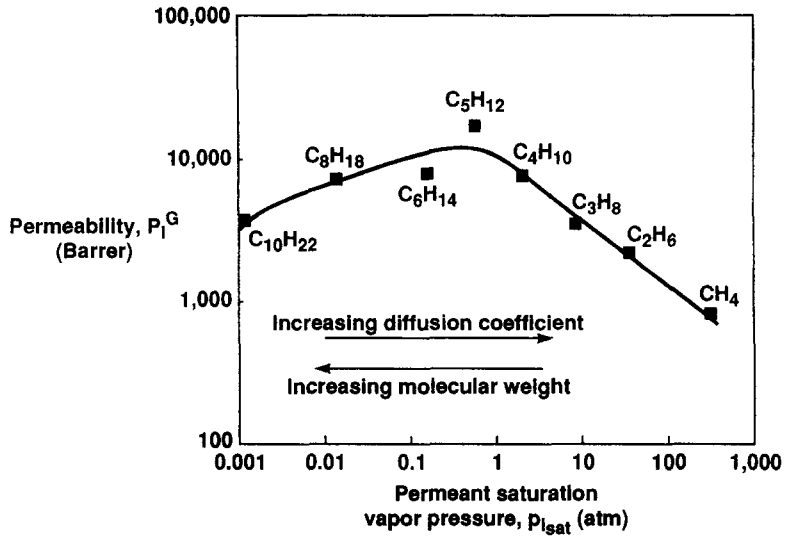

Fig. 6. Permeability coefficient P_i^G of n-alkanes in polydimethylsiloxane as a function of saturation pressure, $p_{i_{sat}}$. Permeability data from [20].

with increasing molecular weight because $p_{i_{sat}}$ is the dominant term. Above molecular weight 100, the molecular weight term gradually becomes dominant, and permeabilities fall with increasing molecular weight of the permeant.

Some data for permeation of simple alkanes in silicone rubber membranes that illustrate this behavior are shown in Fig. 6 [20]. As the molecular weight increases from CH_4 to C_5H_{12}, the effect of the decrease in $p_{i_{sat}}$ is larger than the effect of increasing size or D_i. Above pentane, however, the trend is reversed.

3.4. Pervaporation

Pervaporation is a separation process in which a multicomponent liquid is passed across a membrane that preferentially permeates one or more of the components. A partial vacuum is maintained on the permeate side of the membrane, so that the permeating components are removed as a vapor mixture. Transport through the membrane is induced by maintaining the vapor pressure of the gas on the permeate side of the membrane at a lower vapor pressure than the feed liquid. The gradients in chemical potential, pressure, and activity across the membrane are illustrated in Fig. 7.

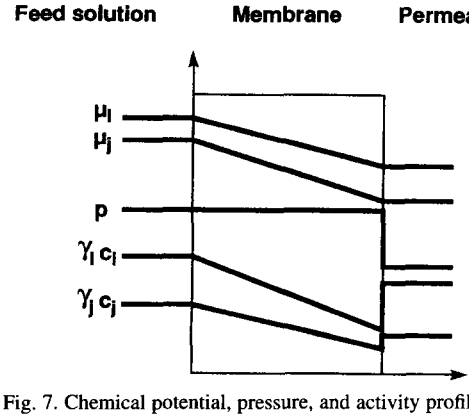

Fig. 7. Chemical potential, pressure, and activity profiles through a pervaporation membrane following the solution-diffusion model.

At the liquid solution/membrane feed interface, the chemical potential of the feed liquid is equilibrated with the chemical potential in the membrane at the same pressure. Eq. (5) then gives

$$\mu_i^o + RT\ln(\gamma_{i_o} c_{i_o}) + v_i(p_o - p_{i_{sat}}) = \mu_i^o + RT\ln(\gamma_{i_{o(m)}} c_{i_{o(m)}}) \cdot v_i(p_o - p_{i_{sat}}) \quad (52)$$

which leads to an expression for the concentration at the feed-side interface

$$c_{i_{o(m)}} = \frac{\gamma_{i_o} c_{i_o}}{\gamma_{i_{o(m)}}} = K_i \cdot c_{i_o} \quad (53)$$

where K_i is the liquid-phase sorption coefficient defined in Eq. (19) in the dialysis and reverse osmosis sections.

At the permeate gas/membrane interface, the pressure drops from p_o in the membrane to p_ℓ in the permeate vapor. The equivalent expression for the chemical potentials in each phase is then

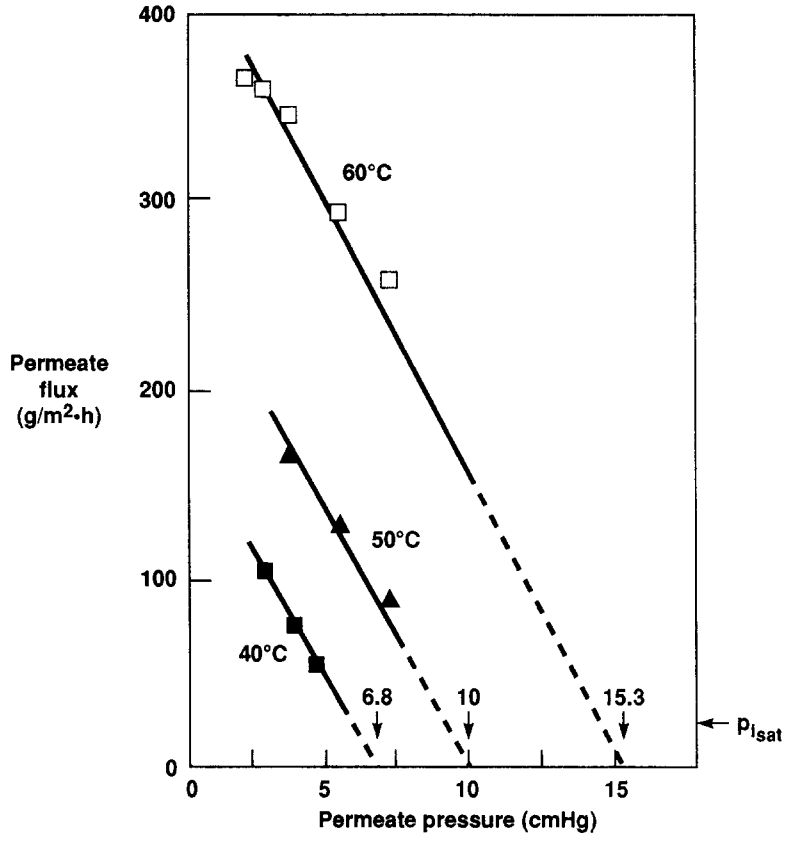

Fig. 8. The effect of permeate pressure on the water flux through a silicone rubber pervaporation membrane. The arrows on the lower axis represent the saturation vapor pressures of the feed solution at the temperature of these experiments.

$$\mu_i^o + RT\ln(\gamma_{i\ell}c_{i\ell}) + RT\ln\left(\frac{p_\ell}{p_{i_{sat}}}\right) = \mu_i^o + RT\ln(\gamma_{i\ell(m)}c_{i\ell(m)}) + v_i(p_o - p_{i_{sat}}) \quad (54)$$

Rearranging Eq. (54) gives

$$c_{i\ell(m)} = \frac{\gamma_{i\ell}}{\gamma_{i\ell(m)}} \cdot \frac{p_\ell}{p_{i_{sat}}} \cdot c_{i\ell} \cdot \exp\left(\frac{-v_i(p_o - p_{i_{sat}})}{RT}\right) \quad (55)$$

As before, the exponential term is close to 1; thus, the concentration at the permeate side interface is:

$$c_{i\ell(m)} = \frac{\gamma_{i\ell}}{\gamma_{i\ell(m)}} \cdot c_{i\ell} \cdot \frac{p_\ell}{p_{i_{sat}}} \quad (56)$$

The product $c_{i\ell} \cdot p_\ell$ can be replaced by the partial pressure term $p_{i\ell}$, thus

$$c_{i\ell(m)} = \frac{\gamma_{i\ell}}{\gamma_{i\ell(m)}} \cdot \frac{p_{i\ell}}{p_{i_{sat}}} = K_i^G \cdot p_{i\ell} \quad (57)$$

where K_i^G is the gas-phase sorption coefficient defined in Eq. (47) in the gas separation section.

The concentration terms in Eqs. (53) and (57) can be substituted into Eq. (11) (Fick's law) to obtain an expression for the membrane flux. However, the sorption coefficient in Eq. (53) is a liquid-phase coefficient whereas the sorption coefficient in Eq. (57) is a gas-phase coefficient. The interconversion of these two coefficients can be handled by considering a hypothetical vapor in equilibrium with feed solution [21]. This vapor–liquid equilibrium can then be written

$$\mu_{i_o} + RT\ln(\gamma_{i_o}^L \cdot c_{i_o}^L) + v_i(p_o - p_{i_{sat}}) = \mu_i^o + RT\ln(\gamma_{i_o}^G \cdot c_{i_o}^G) + RT\ln\left(\frac{p_o}{p_{i_{sat}}}\right) \quad (58)$$

Following the same steps as were taken from Eq. (54) to (57), Eq. (58) becomes

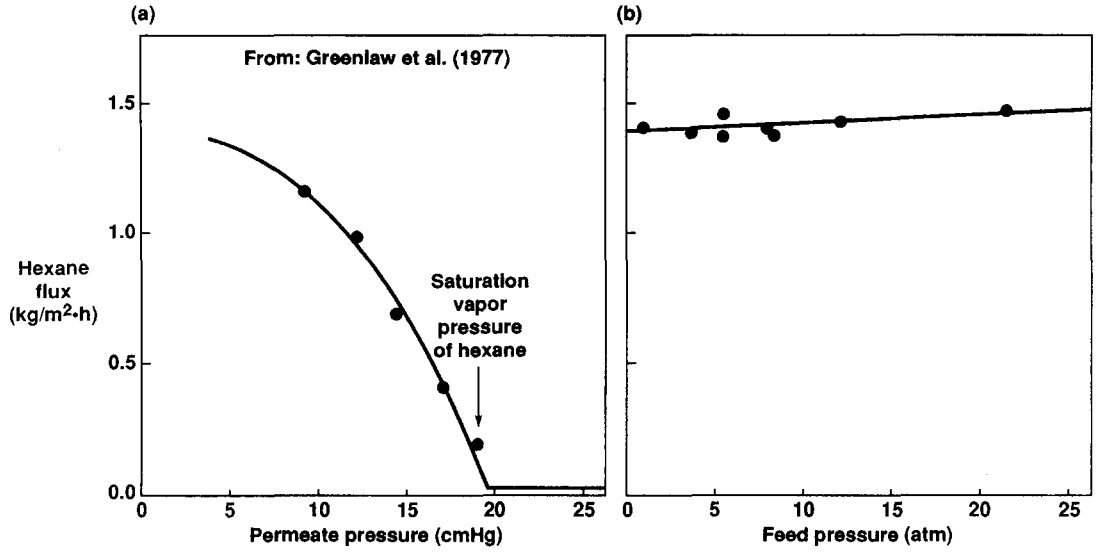

Fig. 9. The effect of feed and permeate pressure on the flux of hexane through a rubbery pervaporation membrane. The flux is essentially independent of feed pressure up to 20 atm but is extremely sensitive to permeate pressure [19]. The explanation for this behavior is the transport Eq. (61).

$$c_{i_o} = \frac{\gamma_{i_o}^G}{\gamma_{i_o}^L \cdot p_{i_{sat}}} p_{i_o} \tag{59}$$

where p_{i_o} is the partial vapor pressure of i in equilibrium with the feed liquid. The term $\gamma_{i_o}^L \cdot p_{i_{sat}} / \gamma_{i_o}^G$ is sometimes referred to as the Henry's law coefficient, H_i. Substitution of Eq. (59) into Eq. (53) yields

$$c_{i_{o(m)}} = \frac{\gamma_{i_o}^G}{\gamma_{i_{o(m)}}} \cdot \frac{p_{i_o}}{p_{i_{sat}}} = K_i^G \cdot p_{i_o} \tag{60}$$

Combining Eqs. (57) and (60) with Eq. (11) gives

$$J_i = \frac{P_i^G}{\ell}(p_{i_o} - p_{i_\ell}) \tag{61}$$

$$= \frac{p_i^G}{\ell}(c_{i_o} \cdot \gamma_{i_o}^L \cdot p_{i_{sat}} / \gamma_{i_o}^G - p_{i_\ell})$$

$$= \frac{P_i^G}{\ell}(c_{i_o} \cdot H_i - p_{i_\ell})$$

From Eq. (59) it follows that

$$K_i = K_i^G \cdot H_i \tag{62}$$

therefore

$$P_i = P_i^G \cdot H_i \tag{63}$$

and, as an alternative to Eq. (61), the flux can be written as

$$J_i = \frac{P_i}{\ell}(c_{i_o} - p_{i_\ell}/H_i) \tag{64}$$

Eq. (61) expresses the driving force in pervaporation in terms of the vapor pressure. The driving force could equally well have been expressed in terms of concentration differences. As a practical matter, however, the use of vapor pressure leads to much more useful results; this has been amply demonstrated experimentally [21,19]. Fig. 8, for example, shows data for the pervaporation of water as a function of permeate pressure. As the permeate pressure (p_{i_ℓ}) increases, the water flux falls, reaching zero flux when the permeate pressure is equal to the feed-liquid vapor pressure (p_{i_o}) at the temperature of the experiment. The straight lines in Fig. 8 indicate that the permeability coefficient of water in silicone rubber is constant. This can be expected in this and similar systems in which the membrane material is a rubbery polymer and the permeant swells the polymer only moderately.

Thompson et al. [19] have studied the effect of feed and permeate pressure on pervaporation flux in some detail. Some illustrative results are shown in Fig. 9. As Fig. 9(a) shows, the dependence of flux on permeate pressure in pervaporation is in accordance with Eq. (61). The flux decreases with increasing permeate pressure, reaching a minimum value when the permeate

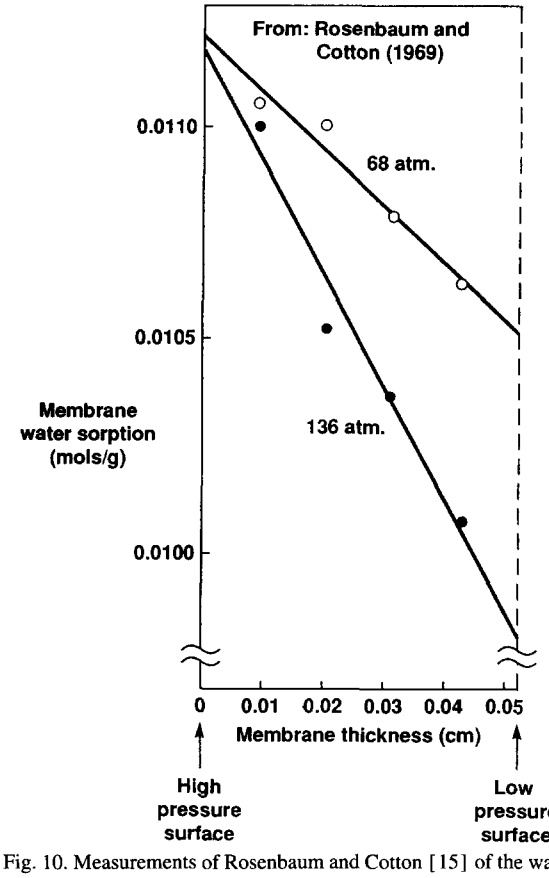

Fig. 10. Measurements of Rosenbaum and Cotton [15] of the water concentration gradients in a laminated cellulose acetate membrane under applied pressures of 68 and 136 atm.

pressure equals the saturation vapor pressure of the feed. The curvature of the line in Fig. 9(a) shows that the permeability coefficient decreases with decreasing permeate pressure, that is, P_{hexane} decreases with a decrease in hexane concentration in the membrane. This behavior is typical of membranes that are swollen significantly by the permeant. If on the other hand, as shown in Fig. 9(b), the permeate pressure is fixed at a low value, the hydrostatic pressure of the feed liquid can be increased to as much as 20 atm without any significant change in the flux. This is because increased hydrostatic pressure produces a minimal change in the partial pressure of the feed liquid partial pressure (p_{i_o}), the true driving force shown in Eq. 57. Thus, the properties of pervaporation membranes illustrated in Fig. 8 and Fig. 9 are easily rationalized by the solution-diffusion model as given above but are much more difficult to explain by a pore-flow mechanism, although this has been tried [22].

4. Evidence for the solution-diffusion model

In the discussion above, the solution-diffusion model was used to derive equations that predict the experimentally observed performance of the membrane processes of dialysis, gas separation, reverse osmosis, and pervaporation. It was not necessary to resort to any additional process-specific model to obtain these results. This agreement between theory and experiment is good evidence for the validity of the solution-diffusion model. Moreover, the large body of permeability, diffusion, and partition coefficient data obtained over the past twenty years for these different processes are in good numerical agreement with one another. This universality and simplicity of the solution-diffusion model are its most useful features and are a strong argument for the validity of the model. Finally, a number of direct experimental measurements can be made to distinguish between the solution-diffusion model and other models, such as the pore-flow model.

One prediction of the solution-diffusion model, controversial during the 1970s, is that the action of an applied pressure on the feed side of the membrane is to *decrease* the concentration of the permeant on the *low-pressure* side of the membrane. This counter-intuitive effect is illustrated in Fig. 1 and Fig. 2. A number of workers have verified this prediction experimentally with a variety of polymer membranes, ranging from diffusion of water in glassy cellulose acetate membranes to diffusion of organics in swollen rubbers [11,15,16]. Convincing examples of this type of experiment are the results of Rosenbaum and Cotton shown in Fig. 10 [15]. In these experiments, four thin cellulose acetate films were laminated together, placed in a high-pressure reverse osmosis cell, and subjected to feed pressures of 68 or 136 atm. The permeate was maintained at atmospheric pressure. After the membrane laminate had reached a steady state, the membrane was quickly removed from the cell, and the water concentration in each laminate measured. As predicted by the solution-diffusion model and shown in Fig. 10, the applied pressure decreases the concentration of water on the permeate side of the membrane. Also, the concentration difference across the membrane

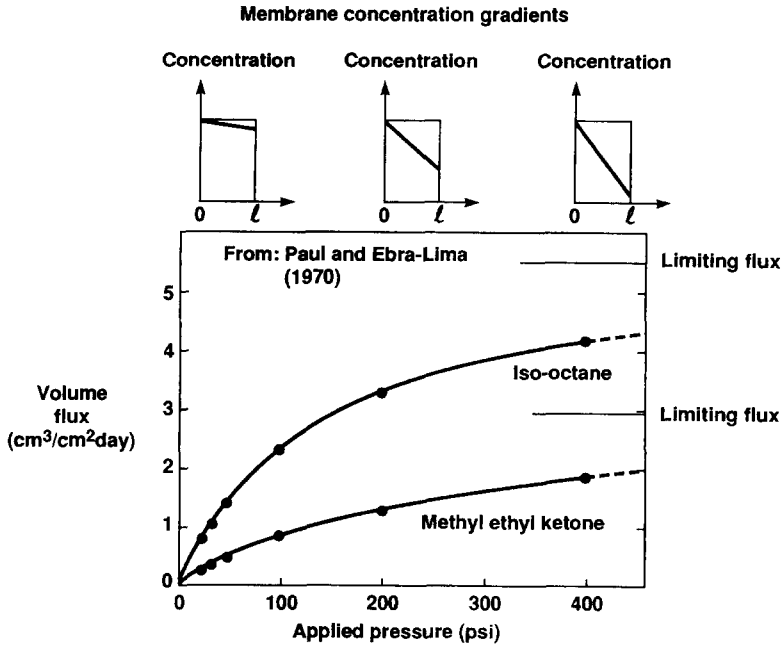

Fig. 11. Pressure permeation (reverse osmosis) of *iso*-octane and methyl ethyl ketone through crosslinked natural rubber membranes 265-μm thick. The change in the concentration gradient in the membrane as the applied pressure is increased is illustrated by the inserts. At high applied pressures, the concentration gradient and the permeation fluxes approach their limiting values [7].

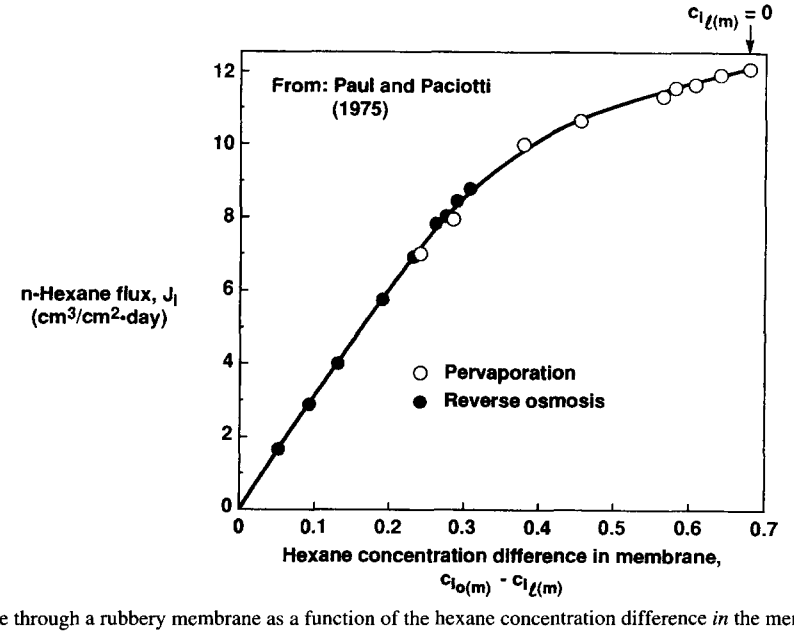

Fig. 12. Flux of *n*-hexane through a rubbery membrane as a function of the hexane concentration difference *in* the membrane. Data taken from both pervaporation (∘) and reverse osmosis (·) experiments. Feed-side and permeate-side membrane concentrations, $c_{io(m)}$ and $c_{i\ell(m)}$ calculated from the operating conditions through Eqs. (65)–(67). Maximum flux is obtained at the maximum concentration difference when the permeate-side membrane concentration, $c_{i\ell(m)}$, equals zero. From Paul and Paciotti [11].

at 136 atm applied pressure is about twice that observed at 68 atm, and the measured concentration on the permeate side is within 20% of the expected value calculated from Eq. (28).

Another series of papers by Paul and co-workers [7–11] focuses on the same phenomenon using rubber membranes and permeation of organic solvents such as hexane, benzene, and carbon tetrachloride. These membranes are highly swollen by the organic solvents and, when operated in reverse osmosis fashion, large gradients develop through the membrane even at relatively modest applied pressures. This means that the concentration in the membrane on the permeate side drops to zero and the flux through the membrane reaches a limiting value as feed pressure is increased. Such data are shown in Fig. 11.

Paul and Paciotti [11] then took this work a step further by measuring the flux of a liquid (hexane) through a membrane both in pervaporation experiments with atmospheric pressure on the feed side of the membrane and a vacuum on the permeate side, and in reverse osmosis experiments with liquid at elevated pressures on the feed side and liquid at atmospheric pressure on the permeate side. The hexane flux obtained in these two sets of experiments is plotted in Fig. 12 against the hexane concentration difference *in* the membrane ($c_{i_{o(m)}} - c_{i\ell(m)}$). These concentrations, $c_{i_{o(m)}}$ and $c_{i\ell(m)}$, were calculated from Eqs. (19), (30) and (56). For permeation of a single compound these equations can be simplified as follows. Reverse osmosis and pervaporation:

$$c_{i_{o(m)}} = \frac{1}{\gamma_{i_{o(m)}}} \tag{65}$$

Reverse osmosis:

$$c_{i\ell(m)} = \frac{1}{\gamma_{i\ell(m)}} \exp\left(\frac{-\nu_i(p_o - p_\ell)}{RT}\right) \tag{66}$$

Pervaporation:

$$c_{i\ell(m)} = \frac{1}{\gamma_{i\ell(m)}} \cdot \frac{p_\ell}{p_{i\text{sat}}} \tag{67}$$

Sorption data were used to obtain values for $\gamma_{i(m)}$. As pointed out by Paul and Paciotti, the data in Fig. 12 show that reverse osmosis and pervaporation obey one unique transport equation, Fick's law. In other words, transport follows the solution-diffusion model. The decrease in the slope of the curve at the higher concentration differences, i.e. at the smaller values for $c_{i\ell(m)}$, reflects a decrease in diffusion coefficient as the swelling of the membrane decreases.

5. The transition region

Although the solution-diffusion model appears to be a reliable method of describing transport in many membranes, it does not apply to ultrafiltration membranes used to separate proteins and other dissolved macromolecules from water. Transport in such membranes appears to be best described by a pore-flow model. Even ultrafiltration membranes able to separate solutes as small as sucrose and raffinose from water have water fluxes 100 times the value that can be obtained by solution-diffusion using reasonable values for the partition and diffusion coefficients of water. The observation that many small solutes have the same permeation rate as water and, hence, no rejection by the ultrafiltration membrane, is also readily rationalized by the filtration-type mechanism of a pore-flow membrane, but it is not easily explained by a solution-diffusion membrane.

The transition between a pore-flow and a solution-diffusion mechanism seems to occur with membranes having very small pores. Membranes that reject sucrose and raffinose but pass all micro-ions are clearly pore-flow membranes, whereas desalination-grade sodium-chloride-rejecting membranes clearly follow the solution-diffusion model [23,24]. Presumably, the transition is in the nanofiltration range, with membranes having good rejections to divalent ions and most organic solutes, but rejection of monovalent ions in the 20–50% range. The same transition range must also exist in gas-permeation membranes.

We believe the difference between pore-flow and solution-diffusion mechanisms lies in the relative permanence of the pores. In a solution-diffusion membrane, free-volume elements (pores) that exist in the membrane are present as statistical fluctuations that appear and disappear in about the same time scale as the motions of the permeants traversing the membrane. In a pore-flow membrane, on the other hand, the free-volume elements (pores) are relatively fixed and do not fluctuate in position or volume on the time scale of permeant motion. The larger the individual free volume

elements (pores), the more likely they are to be present long enough to produce pore-flow characteristics in the membrane. As a rough rule of thumb, the transition between permanent (pore-flow) and transient (solution-diffusion) flow appears to be in the range 5 to 10 Å diameter.

One interesting example that falls in this transition region is gas permeation through "superglassy" polymers, such as poly(1-trimethylsilyl-1-propyne) (PTMSP) [25,26]. PTMSP has an unusually high void volume, on the order of 25%. Gas permeabilities in PTMSP are orders of magnitude higher than those of conventional, low-free-volume glassy polymers, and are even substantially higher than those of polydimethylsiloxane, for many years the most permeable polymer known. The extremely high free volume provides a sorption capacity as much as ten times that of conventional glasses. More dramatically, diffusion coefficients are 10^3 to 10^6 times greater than those observed in conventional glassy polymers [27,28]. This combination of extraordinarily high permeabilities, together with the very high free volume, hint at a pore-flow contribution. Nonetheless, the ratio of the diffusion coefficients of oxygen and nitrogen (D_{O_2}/D_{N_2}) is 1.4, a small number for a glassy polymer but still more than would be expected for a simple pore-flow membrane.

PTMSP also has very unusual permeability characteristics with mixtures of condensable and non-condensable gases. For example, the presence of as little as 1% Freon-11 ($CFCl_3$) in nitrogen lowers the nitrogen permeability of PTMSP more than 20-fold from the pure nitrogen permeability [29]. The best explanation for these unusual vapor permeation properties is to propose that PTMSP, because of its very high free volume, has passed from being a polymer film with a distribution of transient free volume elements to an ultra-microporous membrane in which pore-flow transport occurs [25,26]. The transport mechanism involved is then similar to that suggested by Barrer et al. [30,31] in the 1960s and 70s to rationalize gas flow in very finely microporous carbon membranes. According to this mechanism, the condensable vapor ($CFCl_3$) absorbs onto the walls of the small pores, eventually producing capillary condensation in which the pores are partially or completely blocked by the absorbed vapor. This blockage then prevents the flow of the noncondensed gases (nitrogen) through the membrane.

6. Conclusions

The solution-diffusion model is a good description for the transport through dialysis, reverse osmosis, gas separation, and pervaporation membranes. The fundamental equations describing transport in all of these processes can be derived from simple, basic principles without resource to process-specific factors. These equations provide an accurate description of the behavior of these membranes and the dependence of membrane transport on pressure, concentration and the like. The general agreement of transport coefficients derived in all of these processes with each other and the general universality of the approach are strong indications of the models reliability. Direct measurements of concentration gradients in membranes provide additional support for the model.

7. List of symbols

Subscripts i, j refer to components i and j Subscript m refers to the membrane phase Subscript o, and ℓ refer to the feed and permeate interfaces Thus $c_{i\ell(m)}$ means the concentration of component i in the membrane phase m at the permeate interface, ℓ, and $c_{i\ell}$ means the concentration of component i in the fluid at the permeate interface.

A	water permeability constant [Eq. (37)]
B	salt permeability constant [Eq. (41)]
c_i, c_j	mole concentration of components i and j
D_i, D_j	Fick's law diffusion coefficient [Eq. (11)]
H	Henry law coefficient [Eq. (61)]
J_i, J_j	membrane flux
K_i, K_j^L	liquid phase/membrane phase sorption coefficient [Eq. (20)]

K_i^G	gas phase/membrane phase sorption coefficient [Eq. (47)]
k	Darcy's law coefficient [Eq. (8)]
L_i	coefficient [Eq. (1)]
ℓ	membrane thickness
p	pressure
p_o, p_ℓ	pressure in the fluids at the feed and permeate interfaces
p_i, p_j	partial pressures of components i and j
p_i^o, p_j^o	standard state pressures of components i and j
$p_{iFUNCsat}$, $p_{jFUNCsat}$	saturation vapor pressures of components i and j
P_i, P_j	permeabilities of components i and j
P_i^G, P_j^G	permeabilities of components i and j
P_i^L, P_j^L	permeability of components i and j as defined by Eq. (23)
R	gas constant
$\mathbb{R}$	salt rejection coefficient [Eq. (42)]
T	absolute temperature K
μ_i, μ_j	chemical potential of components i and j [Eq. (2)]
μ_i^o, μ_j^o	standard state chemical potential of components i and j
ν_i	molar volume
$\Delta\pi$	osmotic pressure difference across a semipermeable membrane
γ_i, γ_j	activity coefficients of components i and j

References

[1] S. Sourirajan, Reverse Osmosis, Academic Press, New York, 1970.

[2] E. Glueckauf and P.J. Russell, The equivalent pore radius of dense cellulose acetate membranes, Desalination, 8 (1970) 351.

[3] H. Yasuda and A. Petterlin, Diffusive and bulk flow transport in membranes, J. Appl. Polym. Sci., 17 (1973) 433.

[4] A. Petterlin and A. Yasuda, Comments on the relationship between hydraulic permeability and diffusion in homogeneous swollen membranes, J. Polym. Sci., Polym. Phys. Ed., 13 (1974) 1215.

[5] P. Meares, On the mechanism of desalination by reverse osmosis flow through cellulose acetate membrane, Eur. Polym. J., 2 (1966) 241.

[6] P. Meares, J.B. Craig and J. Webster, Diffusion and flow of water in homogeneous cellulose acetate membranes in J.N. Sherwood, A.Y. Chadwick, W.N. Muire and F.L. Swinton (Eds.), Diffusion Processes, Vol. 2, Gordon and Breach, London, 1972.

[7] D.R. Paul and O.M. Ebra-Lima, Pressure-induced diffusion of organic liquids through highly swollen polymer membranes, J. Appl. Polym. Sci., 14 (1970) 2201.

[8] D.R. Paul, Diffusive transport in swollen polymer membranes, in H.B. Hopfenberg (Ed.), Permeability of Plastic Films and Coatings, Pergamon, New York, 1974.

[9] D.R. Paul, Further comment on the relation between hydraulic permeation and diffusion, J. Polym. Sci., 12 (1974) 1221.

[10] D.R. Paul, J.D. Paciotti and O.M. Ebra-Lima, Hydraulic permeation of liquids through swollen polymeric networks: II Liquid mixtures, J. Appl. Polym. Sci., 19 (1975) 1837.

[11] D.R. Paul and J.D. Paciotti, Driving force for hydraulic and pervaporation transport in homogeneous membranes, J. Polym. Sci., Polym. Phys. Ed., 13 (1975) 1201.

[12] D.R. Paul, The solution diffusion model for swollen membranes, Sep. Purif. Methods, 5 (1976) 33.

[13] H.K. Lonsdale, U. Merten and R.L. Riley, Transport properties of cellulose acetate osmotic membranes, J. Appl. Polym. Sci., 9 (1965) 1344.

[14] U. Merten, Transport properties of osmotic membranes, in Desalination by Reverse Osmosis, MIT Press, Cambridge, MA, 1966.

[15] S. Rosenbaum and O. Cotton, Steady-state distribution of water in cellulose acetate membrane, J. Polym. Sci., 7 (1969) 101.

[16] S.N. Kim and K. Kammermeyer, Actual concentration profiles in membrane permeation, Sep. Sci., 5 (1970) 679.

[17] A. Mauro, Some properties of ionic and non ionic semipermeable membranes, Circulation, 21 (1960) 845.

[18] F. Theeuwes, R.M. Gale and R.W. Baker, Transference, a comprehensive parameter governing permeation of solutes through membranes, J. Membrane Sci., 1 (1976) 3.

[19] F.W. Greenlaw, W.D. Prince, R.A. Shelden and E.V. Thompson, The effect of diffusive permeation rates by upstream and downstream pressures, J. Membrane Sci., 2 (1977) 141.

[20] Mempro Company (Division of Oxygen Enrichment Company), Product Data Sheet, 1991.

[21] J.G. Wijmans and R.W. Baker, A simple predictive treatment of the permeation processes in pervaporation, J. Membrane Sci., 79 (1993) 101.

[22] T. Okeda and T. Matsuura, Theoretical and experimental study of pervaporation on the basis of pore flow mechanism, in R. Bakish (Ed.), Proc. Sixth Int. Conf. Pervaporation Chem. Ind., Ottawa, Canada, September 1992, Bakish Materials Corp., P.O. Box 148, Engelwood, NJ.

[23] R.W. Baker, F.R. Eirich and H. Strathmann, Low pressure ultrafiltration of sucrose and raffinose solutions with anisotropic membranes, J. Phys. Chem., 76 (1972) 238.
[24] G. Thau, R. Bloch and O. Kedem, Water transport in porous and nonporous membranes, Desalination, 1 (1966) 129.
[25] R. Srinivasan, S.R. Auvil and P.M. Burban, Elucidating the mechanism(s) of gas transport in poly[1-(trimethylsilyl)-1-propyne] (PTMSP) membranes, J. Membrane Sci., 86 (1994) 67.
[26] L.G. Toy, I. Pinnau and R.W. Baker, Gas separation processes, U.S. Pat. 5,281,255 (25 January 1994).
[27] L.C. Witchey-Lakshmanan, H.B. Hopfenberg and R.T. Bhern, Sorption and transport of organic vapors in poly[(trimethylsilyl)-1-propyne], J. Membrane Sci., 48 (1990) 321.
[28] Y. Ichiraku, S.A. Stern and T. Nakagawa, An investigation of the high gas permeability of poly(trimethylsilyl-1-propyne), J. Membrane Sci., 34 (1987) 5.
[29] I. Pinnau and L. Toy, Private communication.
[30] R. Ash, R.M. Barrer and C.G. Pope, Flow of adsorbable gases and vapors in microporous medium, Proc. Royal Soc., 271 (1963) 19.
[31] R. Ash, R.M. Barrer and P. Sharma, Sorption and flow of carbon dioxide and some hydrocarbons in a microporous carbon membrane, J. Membrane Sci., 1 (1976) 17.